ARTICLE

Supplementary information

Wafer-scale Pulsed Laser Deposition of ITO for Solar Cells: Reduced Damage vs Interfacial Resistance

Yury Smirnov,‡ [a] Pierre-Alexis Repecaud,‡[a] Leonard Tutsch, [b] Ileana Florea, [c] Kassio P.S. Zanoni,[d] Abhyuday Paliwal,[d] Henk J. Bolink, [d] Pere Roca i Cabarrocas, [c] Martin Bivour [b] and Monica Morales-Masis [a]*

Affiliations

a. *MESA+ Institute for Nanotechnology, University of Twente, Enschede, AE 7500, Netherlands*

b. *Fraunhofer Institute for Solar Energy Systems ISE, 79110 Freiburg, Germany*

c. *LPICM, École Polytechnique, CNRS, Institut Polytechnique de Paris, Palaiseau 91120, France*.

d. *Instituto de Ciencia Molecular, Universidad de Valencia, C/ Catedrático J. Beltrán 2, 46980 Paterna, Spain*

‡ These authors contributed equally.

Contacts

m.moralesmasis@utwente.nl

Structural properties of PLD-grown ITO at different pressure conditions

Fig. S1 displays grazing incidence X-ray diffraction (XRD) patterns of the ITO films deposited on glass (Fig. S1(a)) and a-Si:H coated Si wafers (Fig. S1b) at the three deposition conditions before and after the annealing step.

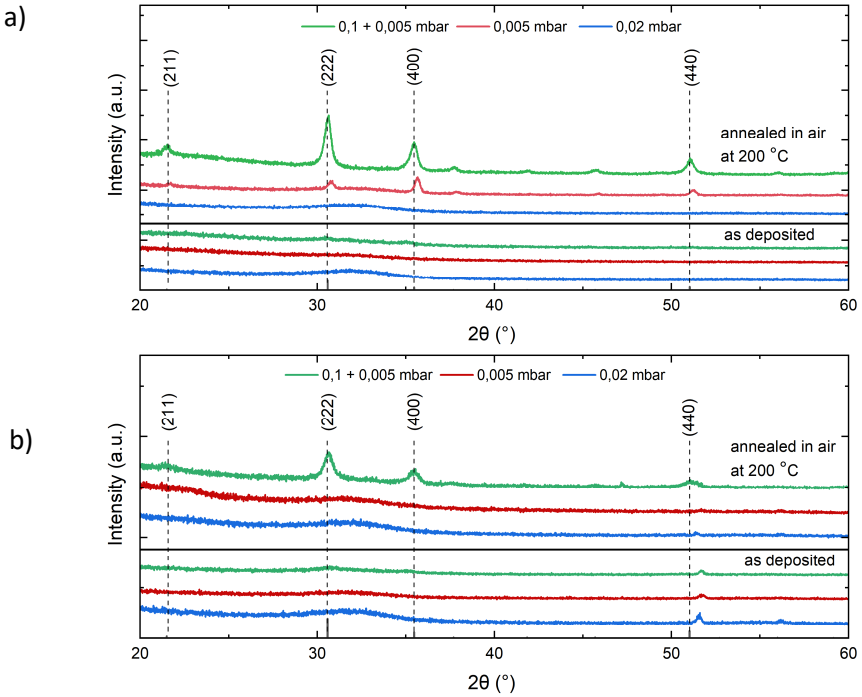

Figure S1: Grazing Incidence XRD (GI-XRD) measurements of the ITO films grown at the three conditions: a) on glass; b) on a-Si:H/c-Si wafers.

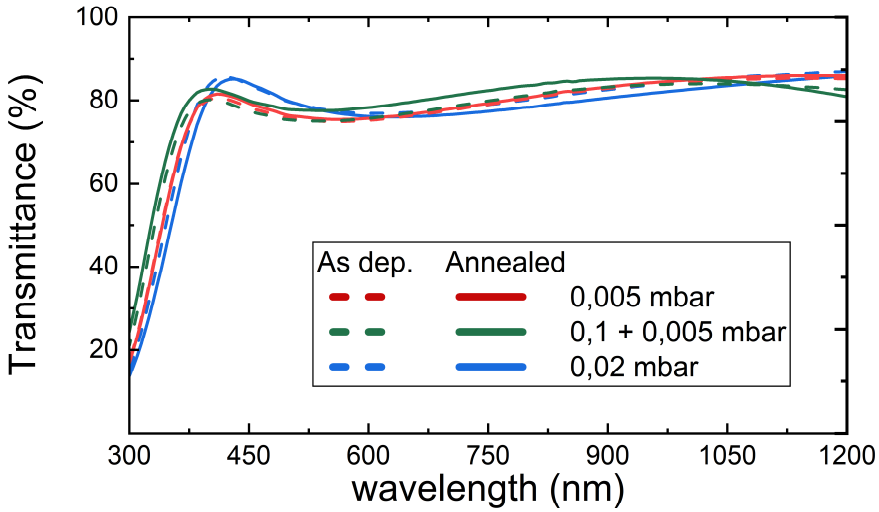

Figure S2: Total transmittance as a function of wavelength for the ITO films grown at the three conditions.

Effect of PLD ITO deposition pressure on buffer-free semi-transparent perovskite solar cells

Figure S3 displays statistical distribution of the main solar cell parameters for devices with different rear ITO electrodes (HP and LP with buffer) for the forward and reverse scan directions measured from the glass side. No hysteresis is observed for the measured devices.

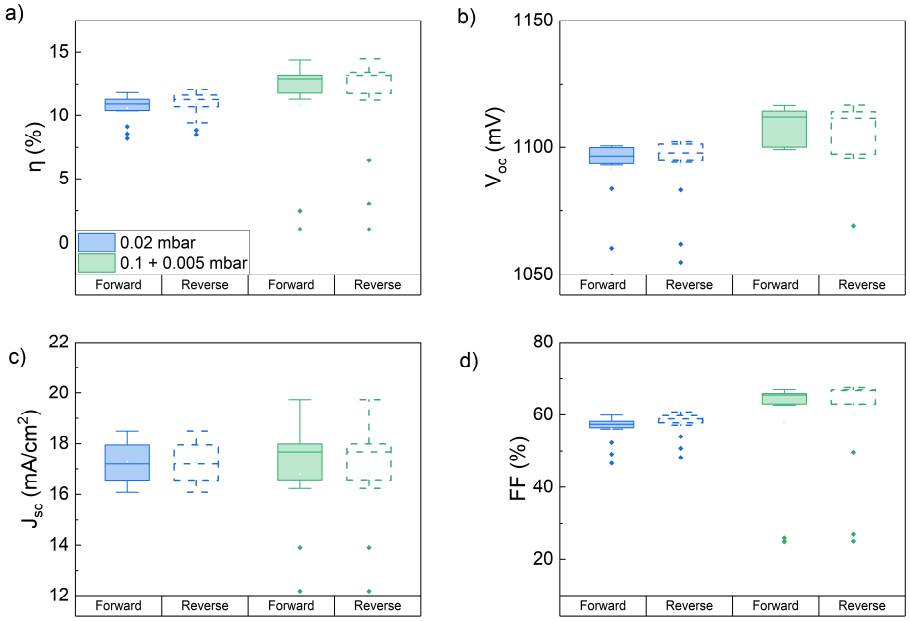

Figure S3: Statistical distribution of solar cell parameters for semi-transparent perovskite devices with the different PLD ITO deposition pressure conditions (0.1 + 0.005 and 0.02 mbar) in forward and reverse scan directions. a) Power conversion efficiency, b) open-circuit voltage (V_{oc}), c) Short-circuit density (J_{sc}), d) fill factor (FF).

Parasitic oxide at a-Si:H/TCO interface as the source of high series resistance

Figure S4 shows the ToF-SIMS profile measurements for samples with ITO by PLD at different pressure conditions: 0.005 mbar (100% O_2 background gas) denoted as the low pressure (LP) and a condition consisting of a very thin (~2 nm) buffer layer deposited at 0.1 mbar (100% O_2) followed by the LP process denoted as LP with buffer. The TCO/a-Si:H interface was defined by the decrease of the In^- and Sn^- signals and the subsequent increase of the Si^- signal. $SiHO_2^-$ and SiO_3In^- signals were integrated using pseudo-voigt function. The mismatch of the peak positions for Si^- and H^- signals for the case of LP ITO (Fig. S4(a,c)) is likely a measurement artefact due to different sputter parameters during ToF-SIMS analysis. The corresponding full width at half maximum (FWHM) and area of the $SiHO_2^-$ and SiO_3In^- signals are summarized in Table S1.

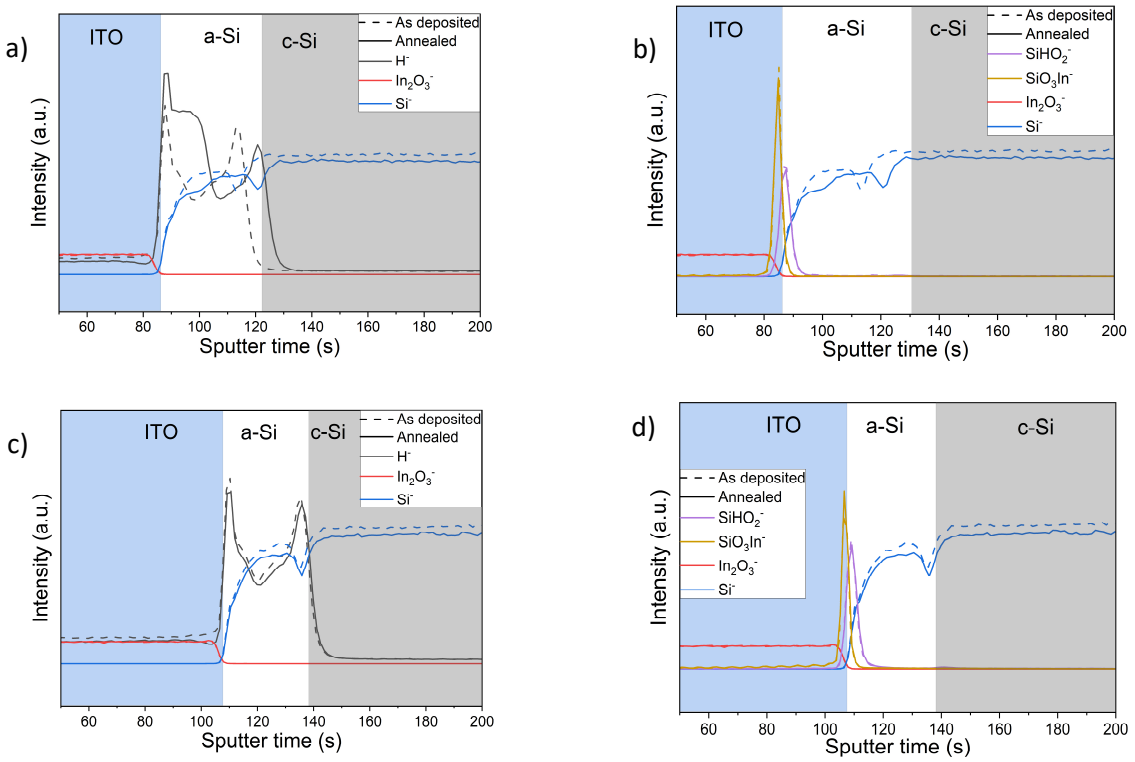

Figure S4: Cross-sectional ToF-SIMS analysis of ITO on SHJ solar cell stack before and after annealing. Signals plotted next to Si^-, $In_2O_3^-$ signals to define the ITO/a-Si interface. a) H^- signal for LP ITO, b) $SiHO_2^-$ and SiO_3In^- signals for LP ITO, c) H^- signal for LP with buffer ITO, b) $SiHO_2^-$ and SiO_3In^- signals for LP with buffer ITO. Integrated ToF-SIMS intensity profiles for c) $SiHO_2^-$ and d) SiO_3In^- signals are indicative of oxygen presence.

Table S1: Full width at half maximum and area of the $SiHO_2^-$ and SiO_3In^- signals

ITO condition	Annealing	**$SiHO_2^-$**		**SiO_3In^-**	
		FWHM (s)	Area (a.u.)	FWHM (s)	Area (a.u.)
0.005 mbar	as deposited	3,65	0,15	2,33	0,17
	200°C in air	3,86	0,14	2,67	0,17
0.02 mbar	as deposited	3,57	0,13	2,03	0,10
	200°C in air	5,00	0,13	3,80	0,11
0.1 + 0.005 mbar	as deposited	3,65	0,14	2,18	0,12
	200°C in air	3,83	0,14	2,47	0,13

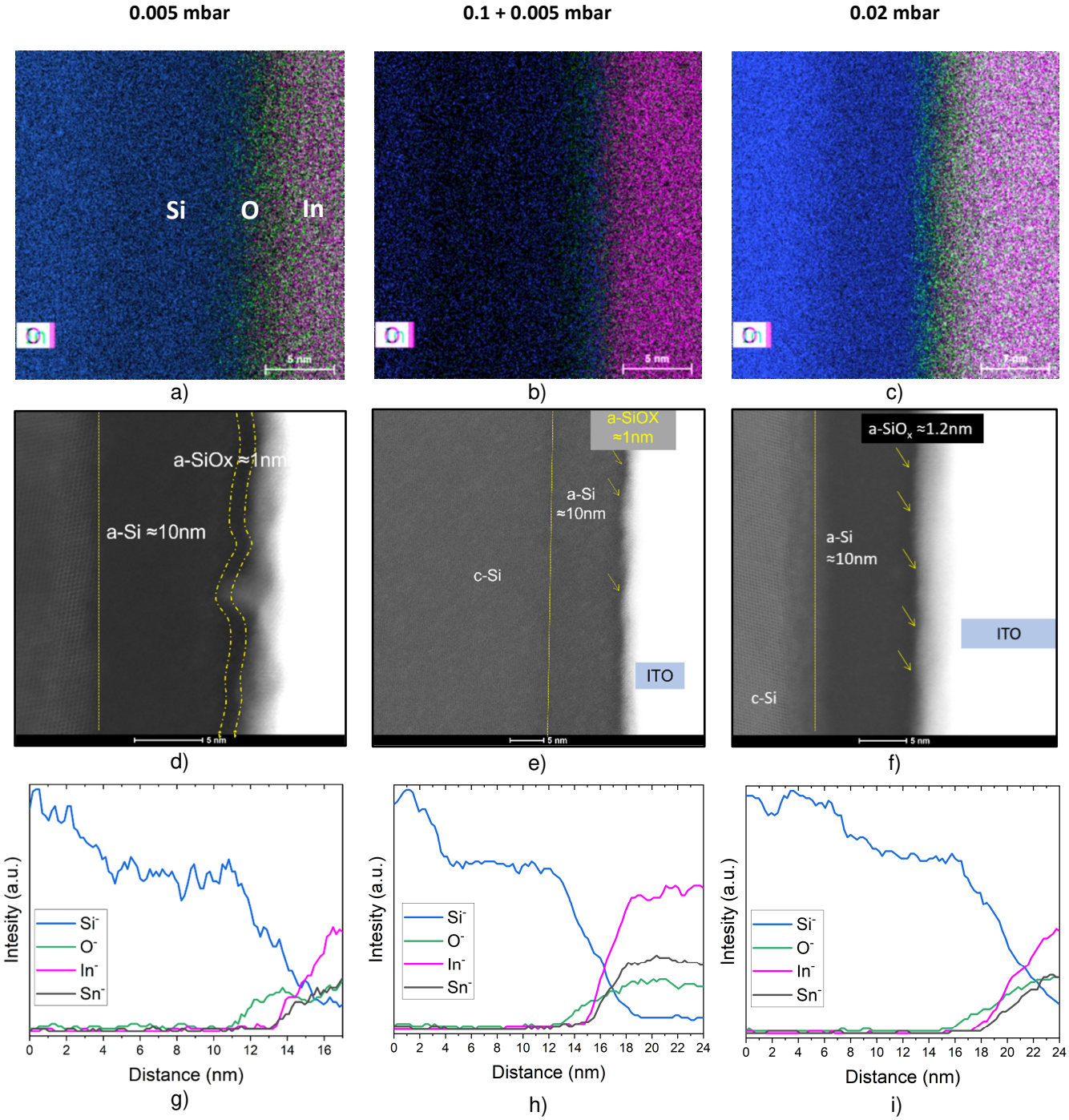

Figure S5: Energy dispersive X-ray chemical mapping of a chosen area of the finished SHJ solar cells after metallization with different ITO by PLD at: a) low pressure; b) low pressure with buffer; c) high pressure. Color code as follows: silicon (blue), oxygen (green), indium (pink). HRSTEM-HAADF images of finished SHJ solar cells after metallization with different ITO by PLD at: a) low pressure; b) low pressure with buffer; c) high pressure. EDX chemical mapping (Fig.S5(a-c)) illustrate the oxygen (green) presence between indium (pink) and silicon (blue) layers. Its presence is given by the low contrast in STEM images next to ITO layer Fig.S5(d-f) with ~1.2 nm thick next to a-Si:H thin layer. EDX line scan profiles across a-Si:H/TCO interface of SHJ cells with different ITO by PLD: g) LP ITO, h) LP with buffer ITO and i) HP ITO. The raise of O^- signal (in green) prior to indium (in pink) and tin (in black) signals is indicative of a parasitic SiO_x formation in the vicinity of a-Si:H/ITO interface. Yellow lines and arrows mark the interface that was inspected for the line scan profile.

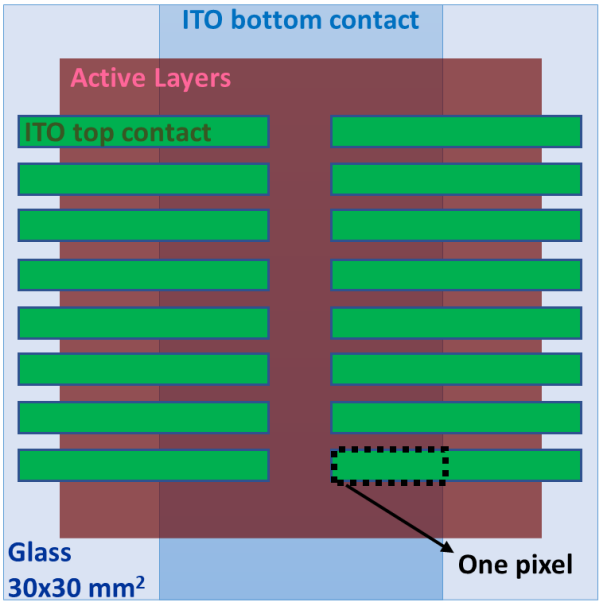

Fig. S6. Device design for the fabricated semi-transparent perovskite solar cell. Each substrate has 16 pixels with active area of 0.0825 cm2, measured using a shadow mask with rectangular wholes concentric to the pixels, with area of 0.0500 cm2.